# Characterization of Photo-Cross-Linked Oligo[poly(ethylene glycol) fumarate] Hydrogels for Cartilage Tissue Engineering

Mahrokh Dadsetan, Jan P. Szatkowski, Michael J. Yaszemski, and Lichun Lu*

*Tissue Engineering and Polymeric Biomaterials Laboratory, Departments of Orthopedic Surgery and Biomedical Engineering, Mayo Clinic College of Medicine, 200 First Street SW, Rochester, Minnesota 55905*

*Received January 16, 2007; Revised Manuscript Received February 27, 2007*

Photo-cross-linkable oligo[poly(ethylene glycol) fumarate] (OPF) hydrogels have been developed for use in tissue engineering applications. We demonstrated that compressive modulus of these hydrogels increased with increasing polymer concentration, and hydrogels with different mechanical properties were formed by altering the ratio of cross-linker/polymer in precursor solution. Conversely, swelling of hydrogels decreased with increasing polymer concentration and cross-linker/polymer ratio. These hydrogels are degradable and degradation rates vary with the change in cross-linking level. Chondrocyte attachment was quantified as a method for evaluating adhesion of cells to the hydrogels. These data revealed that cross-linking density affects cell behavior on the hydrogel surfaces. Cell attachment was greater on the samples with increased cross-linking density. Chondrocytes on these samples exhibited spread morphology with distinct actin stress fibers, whereas they maintained their rounded morphology on the samples with lower cross-linking density. Moreover, chondrocytes were photoencapsulated within various hydrogel networks. Our results revealed that cells encapsulated within 2-mm thick OPF hydrogel disks remained viable throughout the 3-week culture period, with no difference in viability across the thickness of hydrogels. Photoencapsulated chondrocytes expressed the mRNA of type II collagen and produced cartilaginous matrix within the hydrogel constructs after three weeks. These findings suggest that photo-cross-linkable OPF hydrogels may be useful for cartilage tissue engineering and cell delivery applications.

## Introduction

Cartilage has limited capability to regenerate after injury or degenerative arthritis. In the past decade, much research effort in the field of orthopedic tissue engineering has been focused on the development of methods to repair defects in cartilage.[1−3] One challenge is the design and fabrication of biodegradable scaffolds that facilitate specific cellular functions and may thus regulate cell adhesion, proliferation, expression of a specific phenotype, and extracellular matrix (ECM) deposition in a predictable and controlled manner.[4−6] It is known that cell behavior on synthetic polymers is related to the physical and chemical properties of the material, including its composition, surface chemistry, and three-dimensional architecture.[6−8] Scaffold properties may direct cell function through their effect on cell attachment and migration, cell−cell interactions, protein adsorption on the scaffold surface, and diffusion of nutrients and metabolic waste products.[9,10]

Cartilage cells are a useful model for the study of cell−substrate interactions because of the close relationship between chondrocyte morphology and function.[11] This ability arises largely from the cartilage ECM, an abundant network of collagen, proteoglycan, and other molecules. The ECM interacts with chondrocytes through various receptors to modulate chondrocyte metabolism, phenotype, and response to mechanical load.[4,12] Understanding how chondrocytes respond to specific scaffold characteristics would provide insight into strategies that would affect desired cell behavior in regenerative tissue engineering applications.[13,14]

In vitro culture of chondrocytes on substrates in two dimensions has been shown to decrease gene expression and production of cartilage-specific proteins, such as collagen type II and aggrecan, and causes cells to quickly dedifferentiate to a more fibroblastic phenotype.[15] Several researchers have investigated techniques to re-express the chondrogenic phenotype during chondrocyte expansion in monolayer culture by growing cells on microcarriers, by using growth factors such as basic fibroblastic growth factors,[16] or by incorporating cytoskeleton-modifying drugs such as cytochalasin D.[17] However, the effects of material properties on the events that regulate cellular phenotype have not been extensively studied.[6,18]

Various materials have been suggested for use in cartilage repair. These materials have included natural polymers such as collagen,[19] alginate,[20] and hyaluronic acid[21] as well as synthetic polymers such as polyacrylamides,[22] poly(vinyl alcohol),[23] and poly(ethylene glycol) (PEG).[24,25] The advantage of these hydrogels is that they have a high degree of swelling in aqueous environments and thus can promote viability of cells in constructs with a thickness of several millimeters. Oligo[poly(ethylene glycol) fumarate] (OPF) is a novel macromer developed by Jo et al.[26] It has been used for fabrication of hydrogels with a redox initiation system by Temenoff et al.[27] These authors reported that OPF hydrogels are biodegradable and that the mechanical properties and degradation rates of the hydrogels are controlled by the molecular weight of the PEG used in macromer formation. In addition, OPF macromer is composed of biocompatible PEG and fumaric acid. Fumaric acid is a nontoxic carboxylic acid that is part of the Krebs cycle and is used as a food additive. The biocompatibility of pre-cross-linked gels from various OPF formulations and leachable fractions from

* Author to whom correspondence should be addressed. Phone: 507-284-2267. E-mail: lu.lichun@mayo.edu.

10.1021/bm070052h CCC: $37.00 
Published on Web 04/10/2007

related cross-linked hydrogels has been shown in different in vitro and in vivo studies.[28,29] OPF can be cross-linked through the unsaturated double bond in the fumarate group and hydrolytically degraded through its ester bonds. Therefore, this material can provide appropriate properties detailed above for an ideal injectable cell carrier.

In the present study, we used photopolymerization for cross-linking of OPF. Photo-cross-linking provides additional capabilities to potential surgical applications for this and other injectable tissue engineering scaffolds. These advantages include better spatial and temporal control of the polymerization process.[1] For example, consider the treatment of a focal cartilage defect in a knee that has otherwise normal cartilage. After arthroscopic preparation of the defect base and edges, the hydrogel can be injected and molded to fit the defect while still in its viscous, monomeric state, without concern that it will polymerize prematurely. Once the hydrogel, along with any cells and biomolecules it contains, is in the appropriate position, the polymerization process that will maintain its shape and location is started by illuminating the hydrogel with light of the appropriate wavelength. Initiation does not require elevated temperature, and the polymerization rate is sufficiently rapid under physiologic conditions that arthroscopic insertion appears feasible. Photopolymerization has already been used in the microencapsulation of islet cells,[30,31] various controlled-release applications,[32] blood vessel adhesion,[33] and bone restoration.[34] In this work, we used a long-wavelength ultraviolet (UV) light source and a photoinitiator, Irgacure 2959, which has been reported to be cytocompatible.[35] *N*-Vinylpyrrolidinone (NVP) was used as a comonomer and accelerator for photo-cross-linking. NVP acts as a reactive plasticizer that is capable of being cross-linked upon the application of radiation. An accelerating role has been previously reported for NVP in photoencapsulation of pancreatic islet cells.[30]

In this study, we intend to evaluate the characteristics of photo-cross-linked OPF hydrogels as scaffolds for tissue engineering applications. We have determined the mechanical properties and swelling behavior of these hydrogels with varying macromer concentration and NVP ratio. Moreover, we present data showing that changes in hydrogel properties affect adhesion, proliferation, and morphology of chondrocytes cultured on these hydrogels. Photoencapsulation of chondrocytes into OPF hydrogels was also performed, indicating that the process of photo-cross-linking and hydrogel components was not harmful to the cells and they remained viable after cross-linking and during culture. We also demonstrated that photoencapsulated chondrocytes retained their phenotype and were able to produce glycosaminoglycan (GAG) and type II collagen over 21 days in culture.

## Experimental Section

**Materials.** OPF was synthesized from poly(ethylene glycol) (PEG) with an initial molecular weight of 10 000, as previously described.[26] Briefly, 50 g of PEG was azeotropically distilled in toluene to remove residual water and then dissolved in 500 mL of distilled methylene chloride. The resulting PEG was placed in an ice bath and purged with nitrogen for 10 min, and then 0.9 mol of triethylamine (TEA; Aldrich, Milwaukee, WI)/mol of PEG and 1.8 mol of distilled fumaryl chloride (Acros, Pittsburgh, PA)/mol of PEG were added dropwise. The reaction vessel was then removed from the ice bath and stirred at room temperature for 48 h. For purification, methylene chloride was removed by a rotary evaporator. The resulting OPF was dissolved in ethyl acetate and filtered to remove the salt from the reaction of TEA and chloride. OPF was recrystallized in ethyl acetate and vacuum-dried overnight.

**Table 1.** Description of OPF Hydrogels

| hydrogel | OPF:NVP ratio (w/w) |
|---|---|
| N5 | 1:0.05 |
| N10 | 1:0.1 |
| N20 | 1:0.2 |
| N30 | 1:0.3 |

**Gel-Permeation Chromatography.** The molecular weights of the OPF macromer and the PEG used for synthesis were measured with a Waters 717 Plus Autosampler gel-permeation chromatography system (Milford, MA) connected to a model 515 high-performance liquid chromatography pump and model 2410 refractor index detector. Monodispersed polystyrene standards (Polysciences, Warrington, PA) with number-average molecular weights of 474, 6690, 18 600, and 38 000 g/mol and polydispersities of less than 1.1 were used for the calibration curve. Three samples of each material were analyzed.

**Hydrogel Fabrication.** Hydrogels were made by dissolving OPF macromer to final concentrations of 33% and 25% (w/w) in deionized water containing 0.05% (w/w) Irgacure 2959 (Ciba-Specialty Chemicals, Tarrytown, NY) and different concentrations of NVP (Table 1). The macromer solution was pipetted between glass slides with a 1-mm spacer and polymerized with 365 nm UV light (Black-Ray Model 100AP, Upland, CA) at the intensity of approximately 8 mW/cm$^2$ for 10 min.

**Compression Testing.** After cross-linking, hydrogels were cut into disks of 10 mm diameter with a cork borer and swollen in phosphate-buffered saline (PBS, pH 7.4) for 24 h. Compressive modulus of the various swollen hydrogels was determined by use of a dynamic mechanical analyzer (DMA-2980, TA Instruments, New Castle, DE) at a loading rate of 4 N/min. The modulus was determined as the slope of the stress versus strain curve at low strains (<20%).

**Swelling Measurements.** OPF hydrogel disks (10 mm in diameter and 1 mm in thickness) were lyophilized after fabrication, weighed ($W_i$), and swollen in PBS to equilibrium swelling (24 h) at 37 °C. Swollen samples were blotted dry and weighed ($W_s$), then dried under reduced pressure and weighed again ($W_d$). The swelling ratio of the hydrogels was calculated as

$$\text{swelling ratio} = (W_s - W_d)/W_d$$

Sol fraction was calculated for various hydrogels as

$$\text{sol fraction} = (W_i - W_d)/W_i$$

Experiments were conducted three times for both the swelling and sol fraction measurements.

**In Vitro Degradation.** Hydrogel disks were placed in the wells of 12-well tissue culture plates, each containing 2.5 mL of PBS, and incubated at 37 °C on an orbital shaker. PBS was replaced every other day for the first week and weekly thereafter. Swelling ratio of the hydrogels was measured as described at days 7, 14, and 21.

**Cell Culture and Attachment.** ATDC cells (RIKEN Cell Bank, Tsukuba, Ibaraki, Japan) from a clonal mouse chondrogenic cell line were grown to confluence in standard culture flasks in a 1:1 mixture of Dulbecco's modified Eagle medium (DMEM) (Gibco BRL, Rockville, MD) and Ham's F12 medium (Nissui Pharmaceutical Co, Japan), supplemented with 5% fetal bovine serum (Invitrogen, Eugene, OR), 10 $\mu$g/mL human transferrin (Roche, Basel, Switzerland), and 30 nM sodium selenite (Sigma, St. Louis, MO). Cells were maintained in a humidified atmosphere of 5% $CO_2$. Culture medium was changed every 2 days. The cells were then trypsinized and used in experiments.

Swollen hydrogel disks were disinfected with 70% ethanol and washed several times with PBS. Hydrogel films were placed into 24-well tissue culture plates, secured with sterile silicone rubber rings (Cole-Parmer, Vernon Hills, IL), and incubated in DMEM for 24 h prior to cell culture. Suspended chondrocytes were seeded onto the

hydrogels at a density of 20 000 cells/cm$^2$ and incubated at 37 °C. After 4 h, the medium was removed and the plates were rinsed with PBS to remove nonadherent cells, and 1 mL of fresh medium was added. Medium was replaced every 2−3 days. At the desired time points, total number of adherent cells was counted manually from five 20×-objective fields (0.785 mm$^2$) viewed by optical microscope and averaged to determine the cell densities, as previously described.[10] Duplicates of two individual experiments were analyzed for cell densities. Tissue culture polystyrene (TCPS) plates were used as control. The morphology of attached cells was visualized by phase contrast microscopy (Axiovert 25, Carl Zeiss, Inc, Thornwood, NY) equipped with a charge-coupled device camera.

At day 3, cells were stained for actin filaments by fixing in 2% paraformaldehyde for 15 min at room temperature, rinsing twice in PBS, permeabilizing with 0.2% Triton X-100 (Sigma, St. Louis, MO) in PBS for 2 min, and incubating with rhodamine phalloidin (Molecular Probes, Eugene, OR) at final dilution of 1:150 (1.25 units/mL). All samples were mounted with mounting gel including 4′,6′-diamidino-2-phenylindole (DAPI) for nuclei staining and imaged by use of a confocal laser scanning microscope.

**Cell Encapsulation and Viability.** ATDC cells were photoencapsulated in various hydrogel networks ($15 \times 10^6$ cells/mL) by suspending in the desired macromer solution, pipetting into a sterile mold with 1-mm spacers, and polymerization of the hydrogel as described above. The resulting hydrogel−cell constructs were cut into disks of 5 mm diameter, covered with 2.5 mL of culture medium in a 12-well tissue culture plate, and incubated in a humid environment with 5% $CO_2$. To determine the viability of the cells after encapsulation, a live/dead kit (Molecular Probes, Eugene, OR) was used per kit instructions. This technique stains living cells green and dead cells red. After staining, the cells were visualized by confocal scanning microscopy.

**Biochemical Assay for Glycosaminoglycan Production.** Samples from four formulations in Table 1 were removed from the medium after 21 days, rinsed with PBS, homogenized with a pellet grinder, and digested in a solution of 50 $\mu$g/mL proteinase K in 100 mM $K_2HPO_4$, pH 8.0, at 60 °C for 16 h. Proteinase K was then inactivated by heating the solution and digested at 90 °C for 10 min. The preparation was then used for DNA and glycosaminoglycan (GAG) quantification with commercially available assay kits. Total DNA content was measured by the Picogreen cell proliferation kit (Molecular Probes, Eugene, OR) according to manufacturer's directions. Total sulfated glycosaminoglycan content was quantified using the Blyscan glycosaminoglycan assay kit (Biocolor, Newtonabbey, Northern Ireland) according to manufacturer's directions. The GAG content was normalized to the DNA content of each construct.

**RNA Extraction and Preparation.** For gene expression analysis, total RNA from the hydrogel groups was prepared. The samples were homogenized in a tissue sonicator. RNA preparation was carried out with the RNeasy kit (Qiagen, Valencia, CA). Total RNA yields were calculated photometrically.

**Reverse Transcriptase Polymerase Chain Reaction (RT-PCR).** Fifty nanograms of total RNA was reverse-transcribed by use of the iScript cDNA synthesis kit (Bio-Rad Laboratories, Hercules, CA). PCR amplification was carried out in 25-$\mu$L reaction mixtures containing 5 $\mu$L of cDNA, 2.5 $\mu$L of 10× PCR buffer without magnesium (Promega, Madison, WI), 1.5 $\mu$L of 25 mM magnesium chloride (Promega, Madison, WI), 0.25 $\mu$L of AmpliTaq Gold DNA polymerase (Applied Biosystems, Foster City, CA), 2.5 pmol of each primer (Mayo Clinic Laboratories, Rochester, MN), and 0.5 $\mu$L of 10 mM dTTPs (Invitrogen). PCR reaction mixtures were heated to 95 °C for 5 min and then cycled 40 times at 90 °C for 1 min, 60 °C for 1 min, and 72 °C for 1 min. The following primers were used: glyceraldehyde-3-phosphate dehydrogenase (GAPDH) sense sequence 5′-TCCCTCAAGATTGTCAGCAA-3′ and antisense sequence AGATCCACAACGGATACATT-3′, and type II collagen sense sequence 5′-GCCAGACCTGAAACTCTGG-3′ and antisense sequence 5′-GCGATGCTGTTCTTACAGTGG-3′.

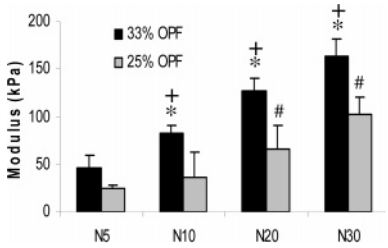


**Figure 1.** Compressive modulus of various oligo[poly(ethylene glycol) fumarate] hydrogels at equilibrium swelling. Data represent mean ± SD ($n = 5$). (*) $p < 0.01$ compared to N5 hydrogel samples with 33% OPF in precursor solution; (#) $p < 0.001$ compared to N5 hydrogel samples with 25% OPF in precursor solution; (+) $p < 0.0001$ compared to the same hydrogel formulation with 25% OPF in precursor solution.

**Immunofluorescence Staining.** Samples were fixed in 2% paraformaldehyde for 20 min and permeabilized in 0.2% Triton X-100 for 2 min. Nonspecific sites were blocked by incubation in 1% bovine serum albumin for 1 h, followed by incubation with mouse anti-chicken collagen type II monoclonal antibody (Chemicon International Inc., Temecula, CA) at room temperature for 1 h. Samples were then rinsed with PBS and incubated in Cy2 conjugated secondary antibody (Chemicon International Inc., Temecula, CA) for 1 h at 37 °C. All samples were mounted with mounting gel including DAPI and imaged by confocal microscopy, with settings adjusted to blacken any residual background fluorescence from the corresponding nonspecific control antibody.

**Statistical Analysis.** All data are reported as mean ± standard deviation (SD) for $n = 3$ except for compressive modulus measurements where $n = 5$. Single-factor analysis of variance (ANOVA) was performed with StatView version 5.0.1.0 (SAS Institute, Inc., Cary, NC) to assess the statistical significance of the results. Bonfferoni's method was employed for multiple comparison tests at significance levels of at least 95%.

## Results

**OPF Synthesis.** Gel-permeation chromatography analysis indicated that the synthesized OPF had a number-average molecular weight ($M_n$) of 9727 ± 1966 and a weight-average molecular weight ($M_w$) of 16 246 ± 3710; PEG used for production of this macromer had an $M_n$ of 9154 ± 466 and an $M_w$ of 11 465 ± 407.

**Hydrogel Fabrication and Characterization.** Hydrogels listed in Table 1 were fabricated by photo-cross-linking of OPF precursor with NVP of varying concentrations in the initial solution (Scheme 1). As these hydrogels are intended for eventual use in sites that must withstand compressive forces, such as the knee, their stiffness was assessed with the measure of compressive modulus. This property shows the ability of the hydrogel to deflect or strain at low pressure. Figure 1 shows that the compressive modulus of OPF hydrogels increased with increasing concentration of NVP in the precursor solutions. Modulus ranged from 25 to 102 kPa for the hydrogels fabricated from 25% weight macromer. An increase in macromer concentration from 25% to 33% weight led to an increase in modulus of the hydrogels. For instance, N30 fabricated from 25% weight macromer had a modulus of 102 kPa, which increased to 163 kPa when the macromer concentration was increased to 33% weight ($p < 0.0001$).

The equilibrium swelling ratios of the various OPF hydrogels are shown in Figure 2. A trend was seen for decreasing hydrogel swelling ratios with increasing concentration of NVP in the initial macromer solution. The equilibrium swelling ratios varied from 27 to 11 for the hydrogels fabricated from 25% weight

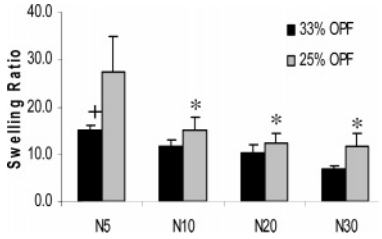


**Figure 2.** Equilibrium swelling ratio of oligo[poly(ethylene glycol) fumarate] hydrogels with variations in macromer and *N*-vinylpyrrolidinone (NVP) concentration. Data represent mean ± SD ($n = 3$). (*) $p < 0.001$ compared to N5 hydrogel samples with 25% OPF in precursor solution; (+) $p < 0.0001$ compared to the same hydrogel formulation with 25% OPF in precursor solution.

**Scheme 1.** Photo-Cross-Linking Reaction for Fabrication of Oligo[poly(ethylene glycol) fumarate] Hydrogels

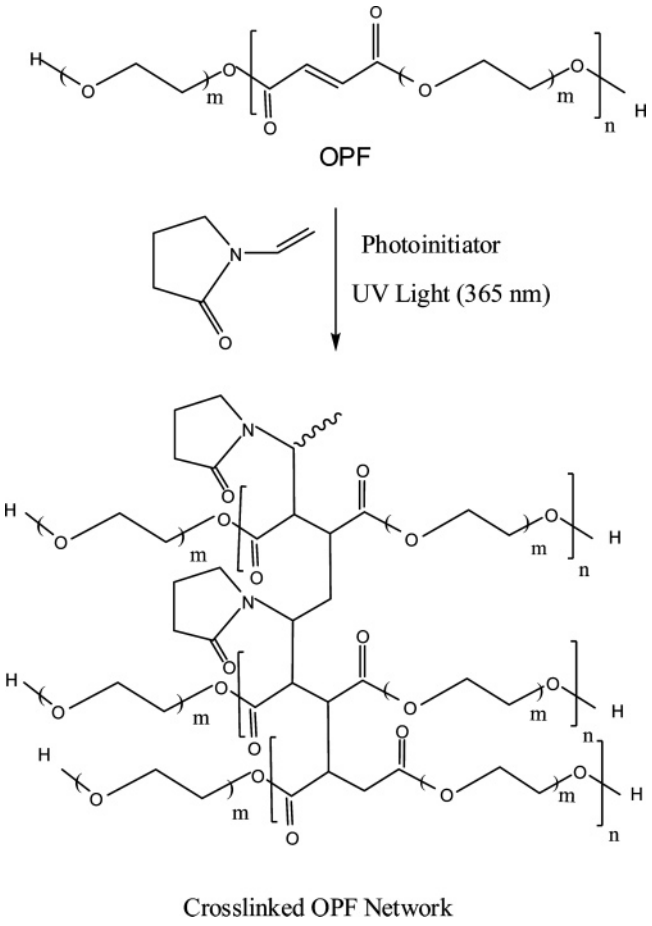


OPF macromer. The swelling ratios decreased when macromer concentration was increased from 25% to 33%, as expected (Figure 2); this decrease in swelling ratio was statistically significant for N5 and N10 ($p < 0.001$). However, differences in swelling ratios of hydrogels with higher NVP concentrations were not statistically significant.

Results from degradation studies in PBS showed that the swelling ratio for hydrogels with lower cross-linking levels (N5 and N10) was constant up to 14 days and then increased dramatically at day 21 (Figure 3 a). This increase in swelling ratio indicated that the hydrogel network began to degrade after 2 weeks. However, the swelling ratio of N20 and N30 remained constant after 21 days, indicating a lower degradation rate for the hydrogels with higher cross-linking levels.

Sol fractions of OPF hydrogels in PBS over time are shown in Figure 3b. Initial sol fraction indicates the percent of non-

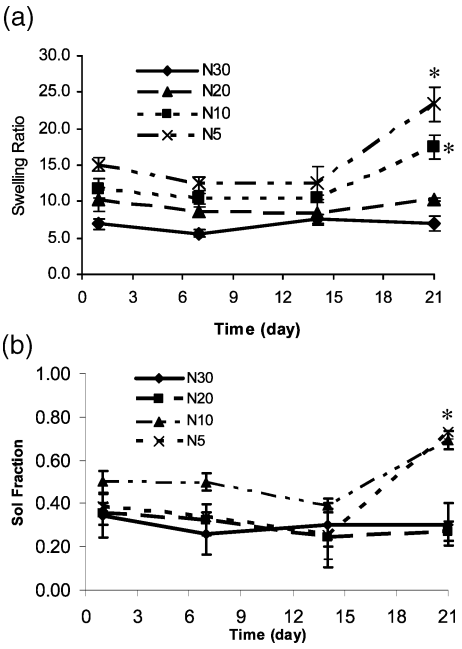


**Figure 3.** Swelling ratio (a) and sol fraction (b) of oligo[poly(ethylene glycol) fumarate] hydrogels in PBS, over 21 days at 37 °C. Data represent mean ± SD ($n = 3$). Swelling ratio and sol fraction of N5 and N10 are greater than N20 and N30 at day 21. (*) $p < 0.05$.

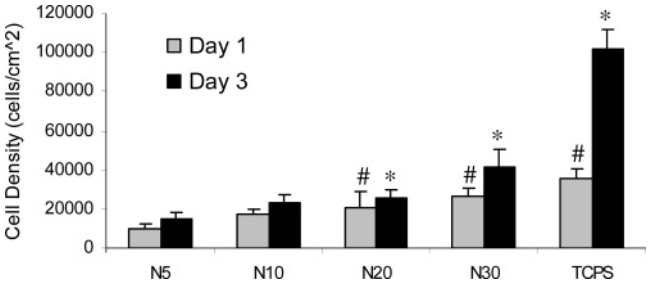


**Figure 4.** Cell density on oligo[poly(ethylene glycol) fumarate] hydrogels along with TCPS after 1 and 3 days in culture. Data represent mean ± SD ($n = 3$). (*) $p < 0.0001$ compared to N5 hydrogel samples at day 3; (#) $p < 0.0001$ compared to N5 hydrogel samples at day 1.

cross-linked macromer. However, increase in sol fraction with time is correlated to the degradation of hydrogels and their weight loss. Similar to swelling ratio, sol fraction of hydrogels remained constant until day 14 and then substantially increased at day 21 for N5 and N10 samples, whereas no difference was seen in sol fraction of N20 and N30 hydrogels over time.

**Cell Attachment and Morphology.** Figure 4 shows ATDC cell densities on OPF hydrogels containing 33% weight macromer with varying cross-linking levels at days 1 and 3 of culture. As seen in this figure, cell attachment was dependent on cross-linking level and increased with increasing NVP cross-linker concentration. Trend for cell density on OPF hydrogels at day 1 was as follows: N5 < N10 < N20 < N30 < TCPS. At day 3, cell densities on all hydrogels were slightly higher than those after 1 day, but the differences were not statistically significant. However, cell density on TCPS greatly increased at day 3. Figure 5 shows representative pictures of chondrocytes on the hydrogels with different cross-linking density after 3 days in monolayer culture. Phase contrast micrographs of adherent chondrocytes (Figure 5a−e) reveal that cells had different morphologies on the surfaces with different cross-linking levels. Cells on N5 and N10 hydrogels had mostly spherical morphol-

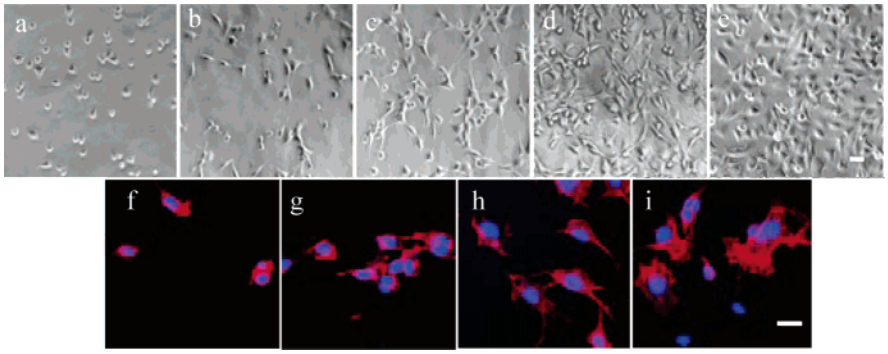


**Figure 5.** ATDC cells seeded on the hydrogel surfaces after 3 days: (a, f) N5, (b, g) N10, (c, h) N20, (d, i) N30, and (e) TCPS. Panels a−e show phase contrast micrographs of the cells at the magnification of ×20. Scale bar = 10 μm. Panels f−i show actin network of the chondrocytes visualized by fluorescently conjugated phalloidin at the magnification of ×40. Scale bar = 10 μm.

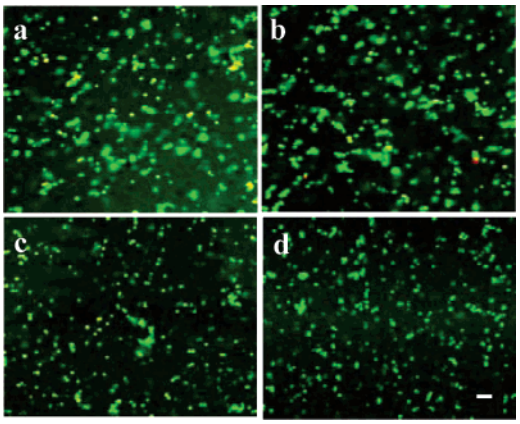


**Figure 6.** Viability of ATDC cells photoencapsulated within oligo[poly(ethylene glycol) fumarate] hydrogels after 21 days in culture: (a) N5, (b) N10, (c) N20, and (d) N30. Live cells are stained green and dead cells are stained red. All magnifications are ×10. Scale bar = 20 μm.

ogy, whereas cells were spread and flattened on samples with increased cross-linking levels. The predominant cell morphology on the N20 and N30 surfaces was a large, flattened cell with stretched fibers similar to fibroblasts. Figure 5f−i shows cellular actin distribution by binding to fluorescence-labeled phalloidin. As seen, chondrocytes attached to the hydrogels with lower cross-linking density were rounded with a diffuse actin network within the cells. However, cells on hydrogels with higher cross-linking density (N20 and N30) exhibited spread morphology with distinct actin stress fibers.

**Cell Viability in OPF Hydrogels.** ATDC cells were encapsulated within N5, N10, N20, and N30 hydrogels fabricated from 33% macromer and examined after 0, 1, 3, 7, and 21 days in culture to determine whether cells survive the photopolymerization process and remain viable during culture in these materials. Viable cells (>95%) were observed throughout the hydrogels at all times during the 21-day culture period (Figure 6). In addition, no differences in viability were noted across the thickness of the hydrogel scaffolds at any time point in the culture period.

**Biochemical Analysis of Glycosaminoglycan.** Biochemical analysis of GAG was performed on encapsulated cells within the constructs and compared as a function of hydrogel composition. Figure 7a shows encapsulated chondrocytes within N5, N10, and N20 constructs produced greater amounts of GAG as compared to N30 with higher cross-linking density ($p < 0.05$). As shown in Figure 7b, DNA content of the constructs with higher cross-linking density (N30) was significantly higher than

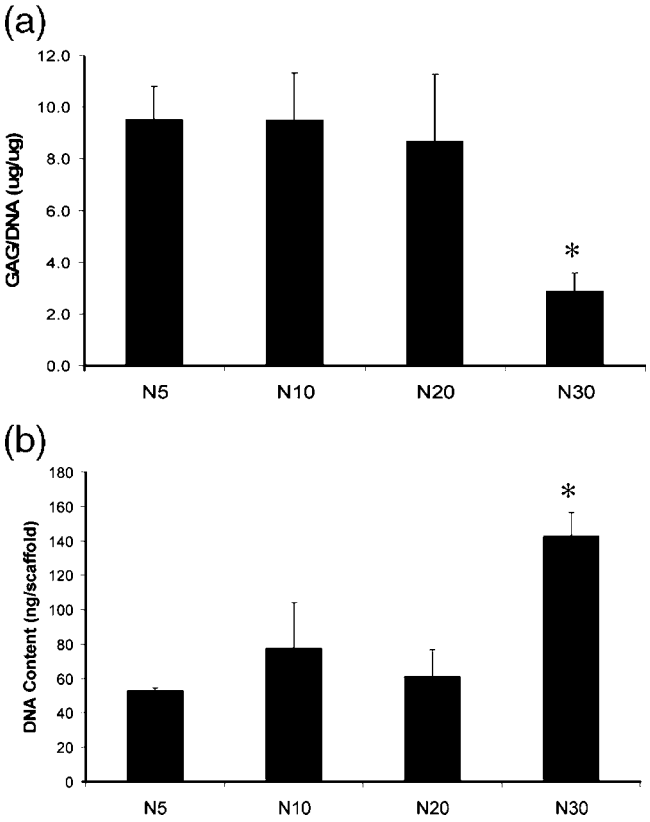


**Figure 7.** Quantification of GAG produced by encapsulated cells into the hydrogels of different formulations after 21 days. (a) GAG content normalized to the DNA content of each construct. Data represent mean ± SD ($n = 3$). (*) $p < 0.05$ compared to the hydrogels of lower cross-linking density. (b) DNA content of the encapsulated cells in each hydrogel scaffold. Data represent mean ± SD ($n = 3$). (*) $p < 0.05$ compared to the hydrogels of lower cross-linking density.

that in constructs with lower cross-linking density, indicating that cells proliferate at a higher rate within this hydrogel formulation.

**Immunofluorescence Staining of Type II Collagen.** Immunofluoresence staining for type II collagen was positive for all hydrogel formulations after 3 weeks of culture, and collagen was mostly localized in the pericellular region of encapsulated cells (Figure 8). However, cells embedded into the N30 constructs appeared to be smaller with condensed collagen near the cell membrane.

**Reverse Transcriptase Polymerase Chain Reaction.** Figure 9 illustrates the continued expression of type II collagen in the hydrogel formulations used in Table 1. The expression level of type II collagen for the given amount of cDNA appears to be

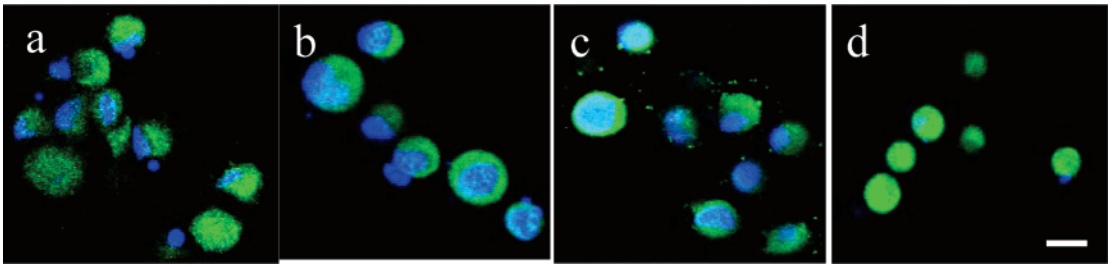


**Figure 8.** Immunofluorescence staining of ATDC cells photoencapsulated within oligo[poly(ethylene glycol) fumarate] hydrogels after 21 days in culture: (a) N5, (b) N10, (c) N20, and (d) N30. All magnifications are ×40. Scale bar = 10 μm.

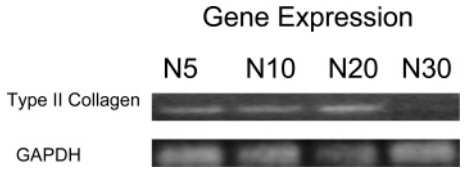


**Figure 9.** RT-PCR analysis for mRNA expression of cartilage-specific matrix protein (type II collagen).

similar on the basis of gel electrophoresis. Our PCR data confirmed that type II collagen gene expression continued at 21 days. All hydrogel formulations showed similar levels of gene expression illustrated by gel electrophoresis of the housekeeping protein GAPDH. However, there was a notable decrease in type II collagen gene expression for the N30 formulation.

## Discussion

To guide cartilage tissue regeneration in vivo, cell scaffolds must be designed to provide the initial mechanical and chemical properties needed in the regeneration location but must simultaneously afford space for tissue deposition that increases with time. In the present study, we aimed to accomplish both design requirements by engineering the mechanical and chemical properties of cross-linked OPF hydrogels. The structural aspects of these OPF networks, especially as a function of degradation rate, were intended to support tissue generation. The results showed that, by varying the percentage of macromer and NVP in solution, the gel properties could be substantially varied. Greater swelling ratios and lower moduli were obtained for hydrogels with lower cross-linking densities. By changing the OPF/NVP ratio in the initial precursor, hydrogels could be formed with compressive modulus ranging from 25 to 163 kPa, that is, about 30% of the compressive modulus of human articular cartilage (530 kPa).[36]

We also showed that the hydrogel degradation rate correlated to the degree of cross-linking. It appears reasonable to assume that the increase in equilibrium swelling over time is due to the hydrogel degradation resulting from hydrolysis of the fumarate ester linkages. This hydrolytic degradation can create open spaces for ECM secretion. The modulation of the hydrogel degradation rates offers an opportunity to match the new tissue generation rate and allow appropriate space for tissue ingrowth while maintaining the mechanical properties of the remaining scaffold.

To evaluate cell attachment on OPF hydrogels for their potential use as tissue engineering scaffolds, we cultured the chondrocytes in monolayers on hydrogels with different formulations listed in Table 1. We hypothesized that hydrogel surface properties and stiffness affect cell morphology and phenotype. In Figures 4 and 5, we showed that cell attachment on hydrogels with higher cross-linking levels was significantly greater than on those with lower cross-linking levels. These observations are consistent with previous findings that chondrocytes attached more rapidly and to a greater degree on stiffer substrates produced by increasing cross-linking density when cultured in monolayers.[4] Stiffer substrates have been reported to direct the cells to a flattened, more spread-out morphology, which is one of the characteristics of chondrocyte dedifferentiation. The precise mechanism for the change in chondrocyte morphology and phenotype on substrates with different stiffness is unclear. Our results revealed that using different amounts of NVP as a cross-linker did not affect total protein adsorption on the hydrogels (data not shown). However, previous reports have shown that the responses of the cells to substrate stiffness most likely originate at cell substrate adhesion sites, where mechanical input is translated into intracellular signals through the associated cytoskeleton or enzyme complexes.[37,38] Compared with the other samples, the N5 hydrogel, with its higher swelling ratio, would be expected to have a greater aqueous phase volume to polymer surface area ratio. This relative decrease in available polymer surface area to physiologic fluid volume may reduce the local surface concentration of adhesion specific proteins, including fibronectin, available for nonspecific adsorption to the hydrogel surface.[4,6] Thus, the round cell morphology on our hydrogels with higher swelling ratios may be due to decreased adsorption of fibronectin, a protein that is generally associated with cell spreading. The characteristic phenotype of differentiated chondrocytes is that of rounded cells, which secrete ECM proteins, such as collagen II and aggrecan, with a diffuse actin microfilament network as seen for the cells cultured on N5 (Figure 5f). Upon attachment to substrates with higher cross-linking density (N20 and N30), however, chondrocytes attained a more flattened morphology, with a reorganization of filamentous actin into distinct stress fibers (Figure 5h,i). It has been previously shown that, during this dedifferentiation toward a more fibroblastic phenotype, type II collagen production is decreased, and it is eventually replaced by type I collagen, with a concomitant decrease or cessation of aggrecan synthesis.[4,6] Mahmood et al.[6] have reported that chondrocytes attached to a polymer substrate containing PEG of different molecular weights expressed different phenotypic functions. They showed that chondrocytes on TCPS and polymers with short PEG chains had a more fibroblastic phenotype, with increased expression of focal adhesion components. However, the actin network in chondrocytes cultured on substrates with longer PEG polymers was diffuse and concentrated near the cell membrane, indicating that the actin organization remained similar to that of differentiated primary chondrocytes.

OPF hydrogels with different formulations were also used to investigate chondrocyte encapsulation, thereby studying the effect of hydrogel formulations on cell viability and phenotype in a three-dimensional model. It has been reported by many

investigators that encapsulation of the chondrocytes into the hydrogels allows them to maintain their rounded morphology and desired phenotype.[4−6] In addition, one of the great advantages of photopolymerizable hydrogels is their ability to form hydrogels in situ from a liquid precursor. If photopolymerizable hydrogels could be used as carriers for chondrocyte transplantation, they would provide several desirable properties. Since hydrogels can be formed in situ from injectable solutions, they can be implanted via arthroscopy/endoscopy or subcutaneous injection, allowing the preparation to adjust to the configuration of donor sites in a minimally invasive manner. Furthermore, in order for this treatment to work, cells must remain viable and retain their phenotype within hydrogels during the cartilage reparative process. We demonstrated that cells remained viable after the photopolymerization process after 3 weeks in culture (Figure 6). Biochemical analysis of GAG showed that encapsulated chondrocytes retained their phenotype and produced the cartilaginous matrix, indicating the feasibility of using OPF hydrogels as a cell carrier for chondrocyte transplantation. However, the cross-linking density of the constructs affects phenotypic expression of the encapsulated chondrocytes. As shown in Figure 7, chondrocytes encapsulated within N5, N10, and N20 constructs produced a greater amount of GAG compared with N30 with higher cross-linking density. DNA content of the N30 constructs was significantly higher than that in constructs with other formulations, indicating that cells proliferate at a higher rate within these hydrogels. A high rate of proliferation, together with lower GAG content, could be a sign of chondrocyte dedifferentiation within N30 constructs. Figure 8 showed that encapsulated cells within all hydrogel formulations retained their rounded morphology and expressed type II collagen. It appears collagen was mostly localized in pericellular regions of the chondrocytes in all formulations; conversely, cells embedded into the N30 constructs seemed to be smaller with concentrated collagen near the cell memberane. RT-PCR revealed similar expression of type II collagen in N5, N10, and N20 constructs. However, there was a notable decrease in type II collagen gene expression for the N30 formulation (Figure 9). These results support our previously described data, shown in Figure 7, that cells produced similar levels of cartilaginous matrix in all hydrogel formulations, while entering a proliferative mode within N30 constructs with less GAG production, indicative of chondrocyte dedifferentiation.

Dedifferentiation of the chondrocytes is a major concern in design and fabrication of cartilage tissue engineered scaffolds. We demonstrated that OPF hydrogels meet many of the requirements for their use as carriers for cell delivery. However, matching their mechanical properties with native cartilage remains a challenge. Increase in cross-linking density improves the mechanical properties of hydrogels; however, cell dedifferentiation is most likely to occur in the hydrogels with a higher level of cross-linking. Although this study provides insight into OPF hydrogel degradation and network properties that impact tissue formation and cell differentiation, further optimization is necessary. By understanding the key parameters for engineering temporal structural changes in hydrogels, these scaffolds may be fine-tuned to match tissue-specific types of growth. Our future studies will aim to fine-tune the strength and degradation rate of these hydrogels, while maintaining their desired effects on cell phenotype and protein expression. This adjustment can be done in a variety of ways, such as changing PEG molecular weight or changing the cross-linker and photoinitiator concentrations. Furthermore, to generate hydrogels that are more clinically acceptable, PEG can be exchanged with slow-degrading triblock copolymers or degradable fibers can be incorporated for reinforcement of the hydrogels without adverse effect on their microstructure.

## Conclusions

We showed that UV light could be used for photo-cross-linking of OPF macromer. Hydrogels with different mechanical and swelling behavior were fabricated by changing the concentration of NVP as the cross-linking agent. We also showed that hydrogels were degradable and that degradation rates varied with the cross-linking level. The change in cross-linking level appears to modulate chondrocyte morphology and phenotype on the OPF hydrogels. Furthermore, the viability of chondrocytes photoencapsulated into the OPF hydrogels remained high after 21 days. This study investigated several scaffold design criteria that affect the differentiation and phenotypic expression of embedded chondrocytes. These hydrogel scaffolds appear to be appropriate candidates for further development in vitro and in vivo, with eventual consideration for potential applications in clinical situations that need the generation of three-dimensional cartilaginous tissues.

**Acknowledgment.** This work was supported by Mayo Foundation and NIH Grants R01 AR45871 and R01 EB003060. We gratefully acknowledge Dr. Shawn O'Driscoll for providing the ATDC cells and Dr. Hsi-Wei Chung and Terry Ruesink for their expertise in the handling and culture of these cells.

## References and Notes

(1) Anseth, K. S.; Metters, A. T.; Bryant, S. J.; Martens, P. J.; Elisseeff, J. H.; Bowman, C. N. *J. Controlled Release* **2002**, *78*, 199.
(2) Bryant, S. J.; Nuttelman, C. R.; Anseth, K. S. *Biomed. Sci. Instrum.* **1999**, *35*, 309.
(3) Burdick, J. A.; Mason, M. N.; Hinman, A. D.; Thorne, K.; Anseth, K. S. *J. Controlled Release* **2002**, *83*, 53.
(4) Genes, N. G.; Rowley, J. A.; Mooney, D. J.; Bonassar, L. J. *Arch. Biochem. Biophys.* **2004**, *422*, 161.
(5) Loty, S.; Sautier, J. M.; Forest, N. *Biorheology* **2000**, *37*, 117.
(6) Mahmood, T. A.; de Jong, R.; Riesle, J.; Langer, R.; van Blitterswijk, C. A. *Exp. Cell Res.* **2004**, *30*, 179.
(7) Dadsetan, M.; Mirzadeh, H.; Sharifi-Sanjani, N.; Daliri, M. *J. Biomed. Mater. Res.* **2001**, *57*, 183.
(8) Dadsetan, M.; Jones, J. A.; Hiltner, A.; Anderson, J. M. *J. Biomed. Mater. Res.* **2004**, *71A*, 439.
(9) Collier, T. O.; Jenney, C. R.; DeFife, K. M.; Anderson, J. M. *Biomed. Sci. Instrum.* **1997**, *33*, 178.
(10) Jones, J. A.; Dadsetan, M.; Collier, T. O.; Ebert, M.; Stokes, K. S.; Ward, R. S.; Hiltner, P. A.; Anderson, J. M. *J. Biomater. Sci., Polym. Ed.* **2004**, *15*, 567.
(11) Miot, S.; Woodfield, T.; Daniels, A. U.; Suetterlin, R.; Peterschmitt, I.; Heberer, M.; van Blitterswijk, C. A.; Riesle, J.; Martin, I. *Biomaterials* **2005**, *26*, 2479.
(12) Sah, R. L.; Kim, Y. J.; Doong, J. Y.; Grodzinsky, A. J.; Plaas, A. H.; Sandy, J. D. *J. Orthop. Res.* **1989**, *7*, 619.
(13) Radin, E. L.; Martin, R. B.; Burr, D. B.; Caterson, B.; Boyd, R. D.; Goodwin, C. *J. Orthop. Res.* **1984**, *2*, 221.
(14) Cooper, C.; McAlindon, T.; Coggon, D.; Egger, P.; Dieppe, P. *Ann. Rheum. Dis.* **1994**, *53*, 90.
(15) Loeser, R. F. *Arthritis Rheum.* **1993**, *36*, 1103.
(16) Martin, I.; Suetterlin, R.; Baschong, W.; Heberer, M.; Vunjak-Novakovic, G.; Freed, L. E. *J. Cell. Biochem.* **2001**, *83*, 121.
(17) Loty, S.; Forest, N.; Boulekbache, H.; Sautier, J. M. *Biol. Cell.* **1995**, *83*, 149.
(18) Papadaki, M.; Mahmood, T.; Gupta, P.; Claase, M. B.; Grijpma, D. W.; Riesle, J.; van Blitterswijk, C. A.; Langer, R. *J. Biomed. Mater. Res.* **2001**, *54*, 47.
(19) Yaylaoglu, M. B.; Korkusuz, P.; Ors, U.; Korkusuz, F.; Hasirci, V. *Biomaterials* **1999**, *20*, 711.
(20) Rowley, J. A.; Madlambayan, G.; Mooney, D. J. *Biomaterials* **1999**, *20*, 45.

(21) Temenoff, J. S.; Mikos, A. G. *Biomaterials* **2000**, *21*, 2405.
(22) Jasionowski, M.; Krzyminski, K.; Chrisler, W.; Markille, L. M.; Morris, J.; Gutowska, A. *J. Mater. Sci. Mater. Med.* **2004**, *15*, 575.
(23) Noguchi, T.; Yamamuro, T.; Oka, M.; Kumar, P.; Kotoura, Y.; Hyon, S.; Ikada, Y. *J. Appl. Biomater.* **1991**, *2*, 101.
(24) Cruise, G. M.; Hegre, O. D.; Lamberti, F. V.; Hager, S. R.; Hill, R.; Scharp, D. S.; Hubbell, J. A. *Cell. Transplant.* **1999**, *8*, 293.
(25) Wallace, D. G.; Cruise, G. M.; Rhee, W. M.; Schroeder, J. A.; Prior, J. J.; Ju, J.; Maroney, M.; Duronio, J.; Ngo, M. H.; Estridge, T.; Coker, G. C. *J. Biomed. Mater. Res.* **2001**, *58*, 545.
(26) Jo, S.; Shin, H.; Mikos, A. G. *Biomacromolecules* **2001**, *2*, 255.
(27) Temenoff, J. S.; Athanasiou, K. A.; LeBaron, R. G.; Mikos, A. G. *J. Biomed. Mater. Res.* **2002**, *59*, 429.
(28) Temenoff, J. S.; Shin, H.; Conway, D. E.; Engel, P. S.; Mikos, A. G. *Biomacromolecules* **2003**, *4*, 1605.
(29) Shin, H.; Quinten Ruhe, P.; Mikos, A. G.; Jansen, J. A. *Biomaterials* **2003**, *24*, 3201.
(30) Cruise, G. M.; Hegre, O. D.; Scharp, D. S.; Hubbell, J. A. *Biotechnol. Bioeng.* **1998**, *57*, 655.
(31) Cruise, G. M.; Scharp, D. S.; Hubbell, J. A. *Biomaterials* **1998**, *19*, 1287.
(32) Lu, S.; Anseth, K. S. *J. Controlled Release* **1999**, *57*, 291.
(33) Dumanian, G. A.; Dascombe, W.; Hong, C.; Labadie, K.; Garrett, K.; Sawhney, A. S.; Pathak, C. P.; Hubbell, J. A.; Johnson, P. C. *Plast. Reconstr. Surg.* **1995**, *95*, 901.
(34) Muggli, D. S.; Burkoth, A. K.; Anseth, K. S. *J. Biomed. Mater. Res.* **1999**, *46*, 271.
(35) Bryant, S. J.; Nuttelman, C. R.; Anseth, K. S. *J. Biomater. Sci., Polym. Ed.* **2000**, *11*, 439.
(36) Hoshikawa, A.; Nakayama, Y.; Matsuda, T.; Oda, H.; Nakamura, K.; Mabuchi, K. *Tissue Eng.* **2006**, *12*, 2333.
(37) Discher, D. E.; Janmey, P.; Wang, Y. *Science* **2005**, *310*, 1139.
(38) Robert, J.; Pelham, J. R.; Wang, Y. *Proc. Natl. Acad. Sci. U.S.A.* **1997**, *94*, 13665.

BM070052H